INL/CON-24-76767-Revision-0

Quantitative Insight to Fission Gas Pores Distribution in Irradiated Annular U-10Zr Metallic Fuel Using Machine Learning

March 2024

Changing the World's Energy Future

Tiankai Yao, Yalei Tang, Fei Xu

Idaho National Laboratory

INL/CON-24-76767-Revision-0

Quantitative Insight to Fission Gas Pores Distribution in Irradiated Annular U-10Zr Metallic Fuel Using Machine Learning

Tiankai Yao, Yalei Tang, Fei Xu

March 2024

Idaho National Laboratory
Idaho Falls, Idaho 83415

http://www.inl.gov

Prepared for the
U.S. Department of Energy
Under DOE Idaho Operations Office
Contract DE-AC07-05ID14517

Quantitative Insight to Fission Gas Pores Distribution in Irradiated Annular U-10Zr Metallic Fuel Using Machine Learning

Yalei Tang, Fei Xu, Shoukun Sun, Daniele Salvato, Fidelma Giulia Di Lemma, Min Xian,

Daniel J. Murray, Colin Judge, Luca Capriotti, Tiankai Yao

Idaho National Laboratory

Outline

- **Introduction - Irradiation of Annular Metallic U-10Zr Fuel**
- **Background - Fission gas pores evolution behavior**
- **Challenges - In the analysis of fission gas pores characteristics**
- **Goal - Quantitative Insight to Fission Gas Pores Distribution**
- **Results**
- **Conclusion**

Irradiation of Annular Metallic U-10Zr Fuel

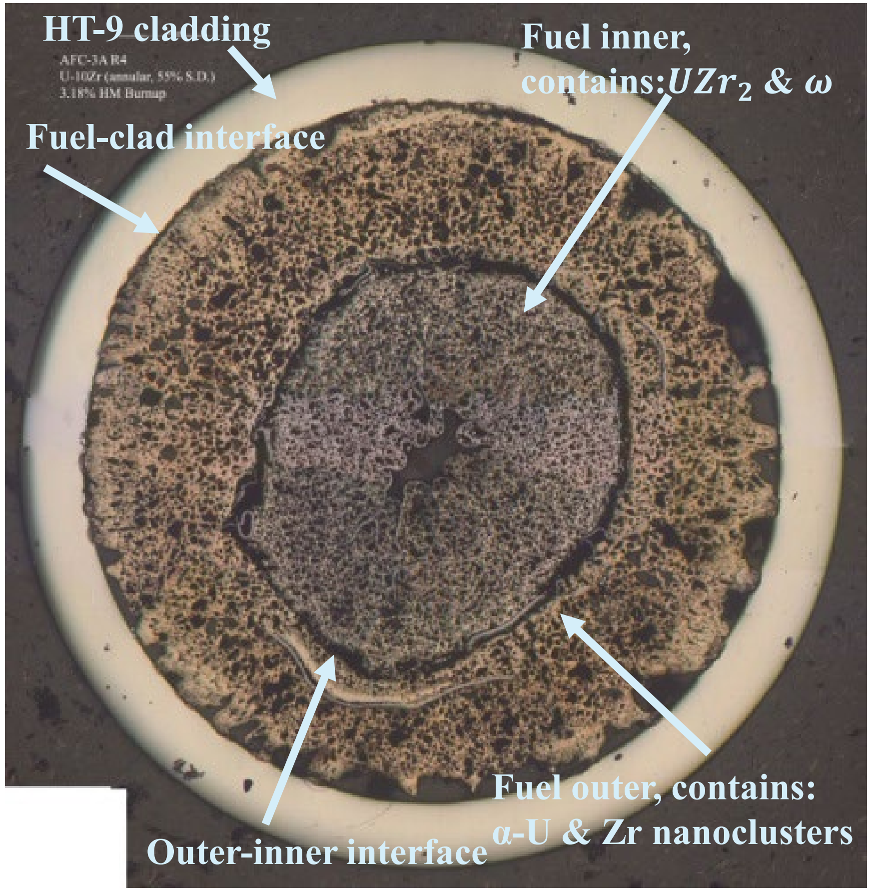

Fig. 1. The optical micrography of a U-10Zr irradiated to 3.3% fission per initial metal atom (FIMA) burnup[1] . Fuel cross section from the irradiated fuel pin at an axial location of x/L=0.5

Annular U-10Zr fuel irradiation conditions

- Designed and fabricated in the Materials & Fuels Complex of Idaho National Laboratory (INL)
- Irradiation experiment carried out in the Advanced Test Reactor (ATR) at INL
- Bonded by Helium (He) and wrapped with HT-9 cladding
- Mounted in epoxy, ground, and polished with sandpaper and diamond paste from 15 micron to 1 micron.

Inner diameter	Outer diameter	Smear density	Burnup rate	Peak inner cladding temperature average	Irradiation days
3.25mm	4.86mm	55%	3.3% FIMA	540 ºC	132 days

References:
1. Cai, L., Xu, F. et al. (2022). Understanding fission gas bubble distribution, lanthanide transportation, and thermal conductivity degradation in neutron-irradiated α-U using machine learning. Materials Characterization.

Fission gas pores evolution behavior

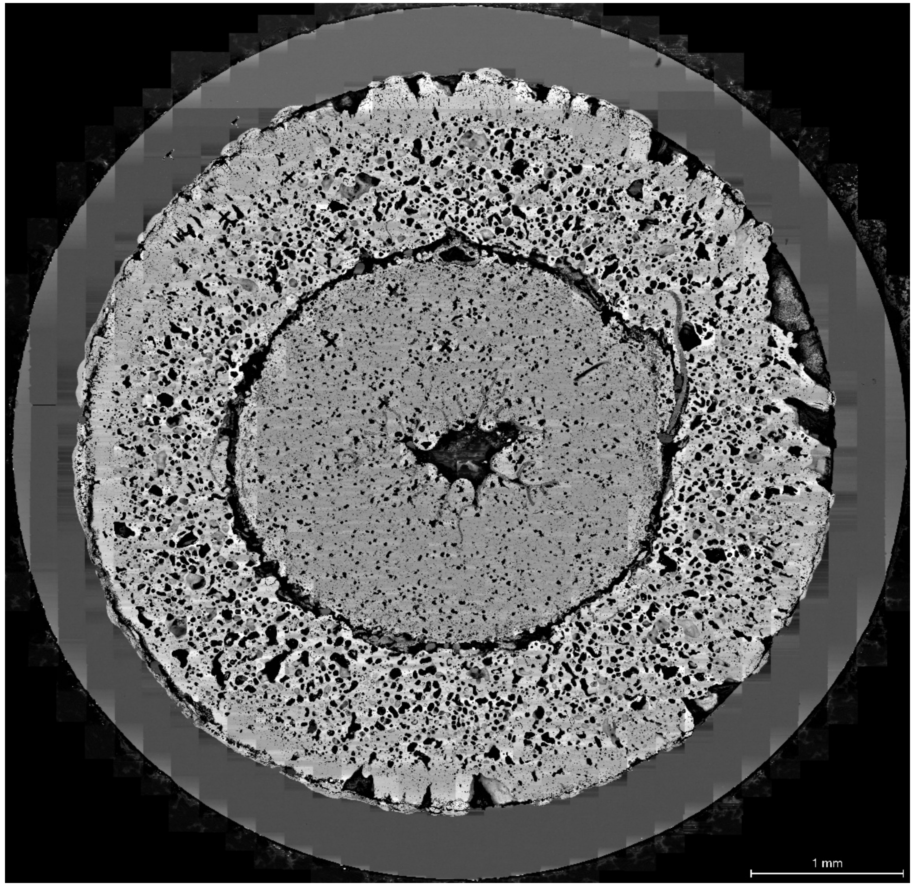

Fig. 1. The Scanning Electron Microscopy (SEM) of a U-10Zr irradiated to 3.3% fission per initial metal atom (FIMA) burnup[1] .

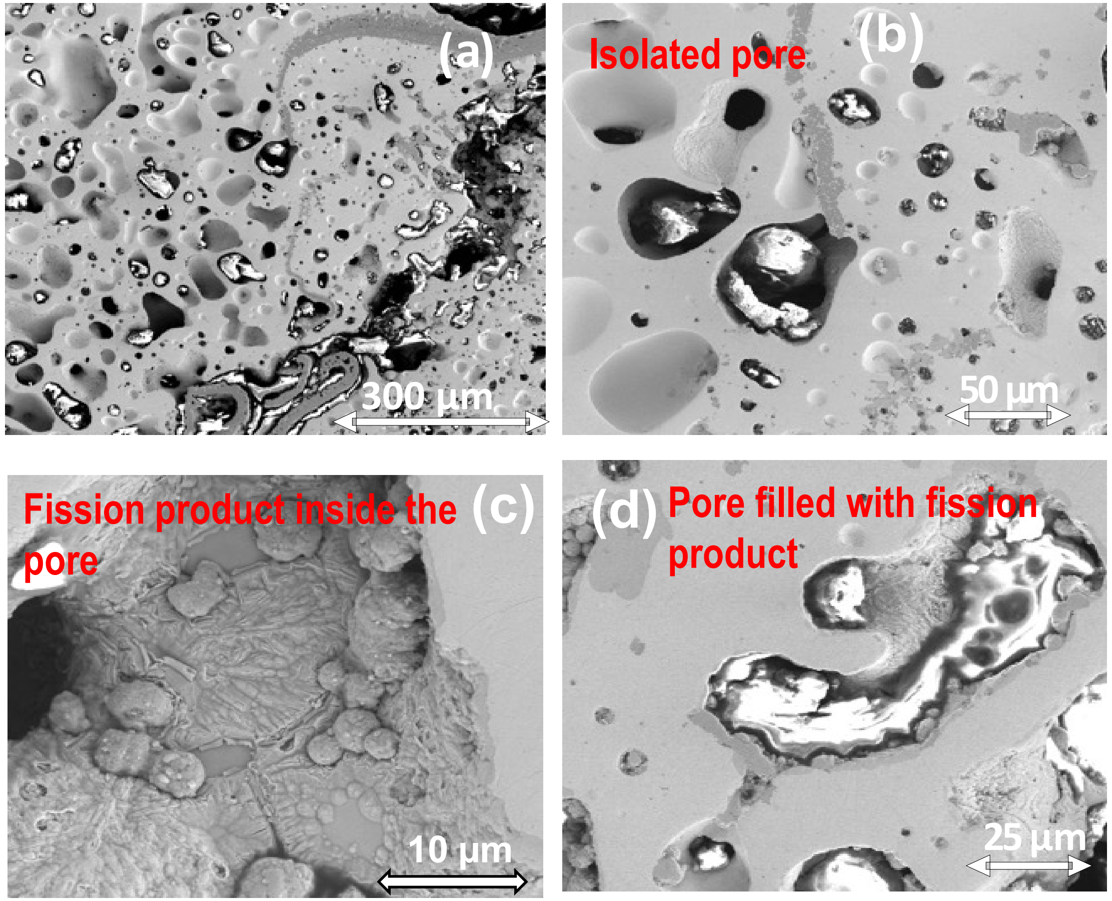

Fig. 2. The SEM images of bubbles in U-10Zr fuel[1] .

References:
1. Cai, L., Xu, F. et al. (2022). Understanding fission gas bubble distribution, lanthanide transportation, and thermal conductivity degradation in neutron-irradiated α-U using machine learning. Materials Characterization.

Challenges in the analysis of fission gas pores characteristics

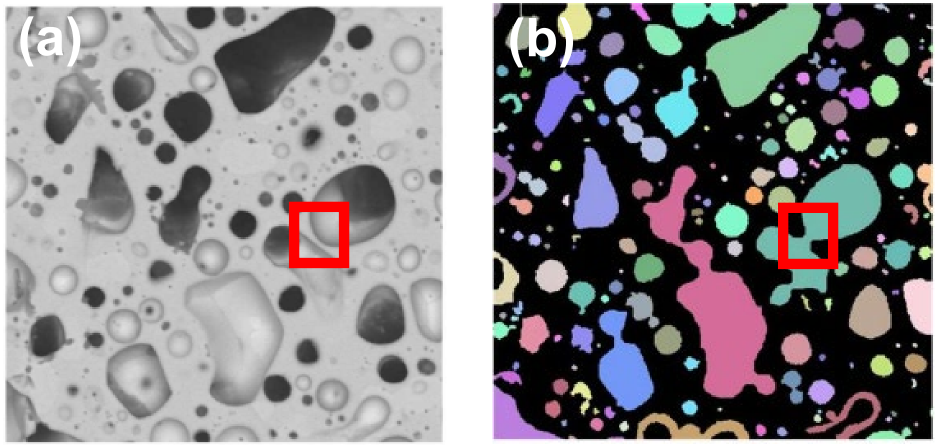

(a) Original image

(b) Bubbles detected using simple threshold method

Fig. 1. Segmentation results using existing segmentation approach on BSE image [19], (a) Original BSE image; (b) Pore boundaries detected using existing segmentation approach. Red boxes show the example that existing method cannot generate accurate boundaries of pores. Purple box shows the model inaccurately detected Pure Zr phase as fission gas pores.

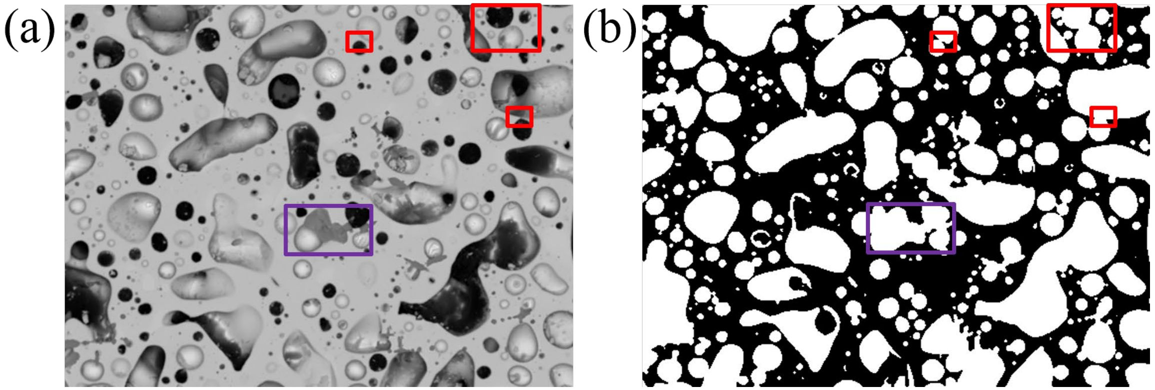

Fig. 2. Segmentation results using existing segmentation approach on BSE image [19], (a) Original BSE image; (b) Pore boundaries detected using existing segmentation approach. Red boxes show the example that existing method cannot generate accurate boundaries of pores. Purple box shows the model inaccurately detected Pure Zr phase as fission gas pores.

Goal

Quantitative Insight to Fission Gas Pores Distribution

1. Fission gas pore segmentation
   - Deep learning model

2. Fission gas pore classification
   - Decision tree model

3. Statistic analysis
   - Pore size
   - Pore shape
   - Pore orientation

Quantitative insight to fission gas pores distribution (1/3)
Fission gas pore segmentation using deep learning model

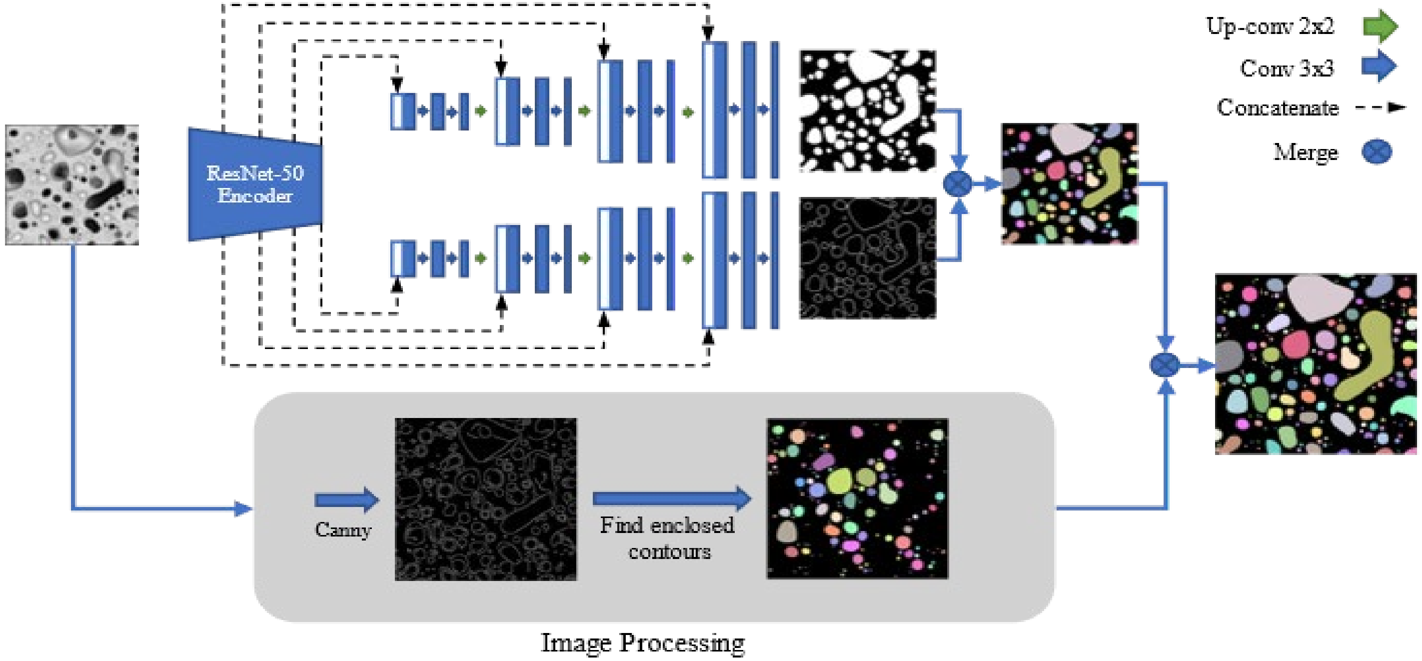

Fig. 1. Pre-trained deep learning model for SEM image segmentation[2] .

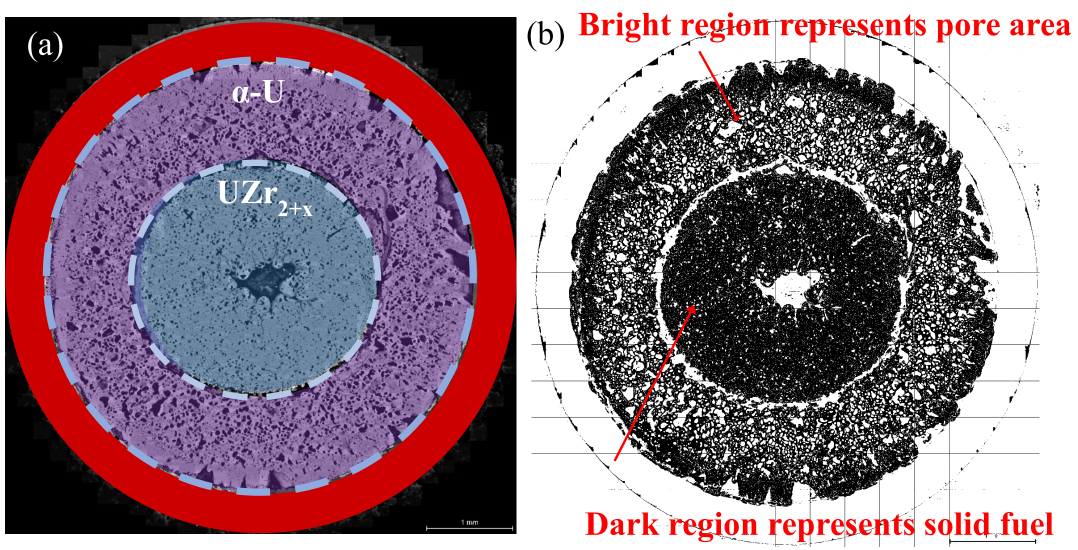

Fig. 2. SEM image segmentation results from the deep learning model, (a) SEM image of U-10Zr fuel cross section; (b) U-10Zr fuel cross section segmented result in binary image.

References:
2. Sun, S., Xu, Fet, al,(2023). An Efficient Instance Segmentation Approach for Studying Fission Gas Bubbles in Irradiated Metallic Nuclear Fuel.

Quantitative insight to fission gas pores distribution (2/3)
Fission gas pore classification using decision tree model

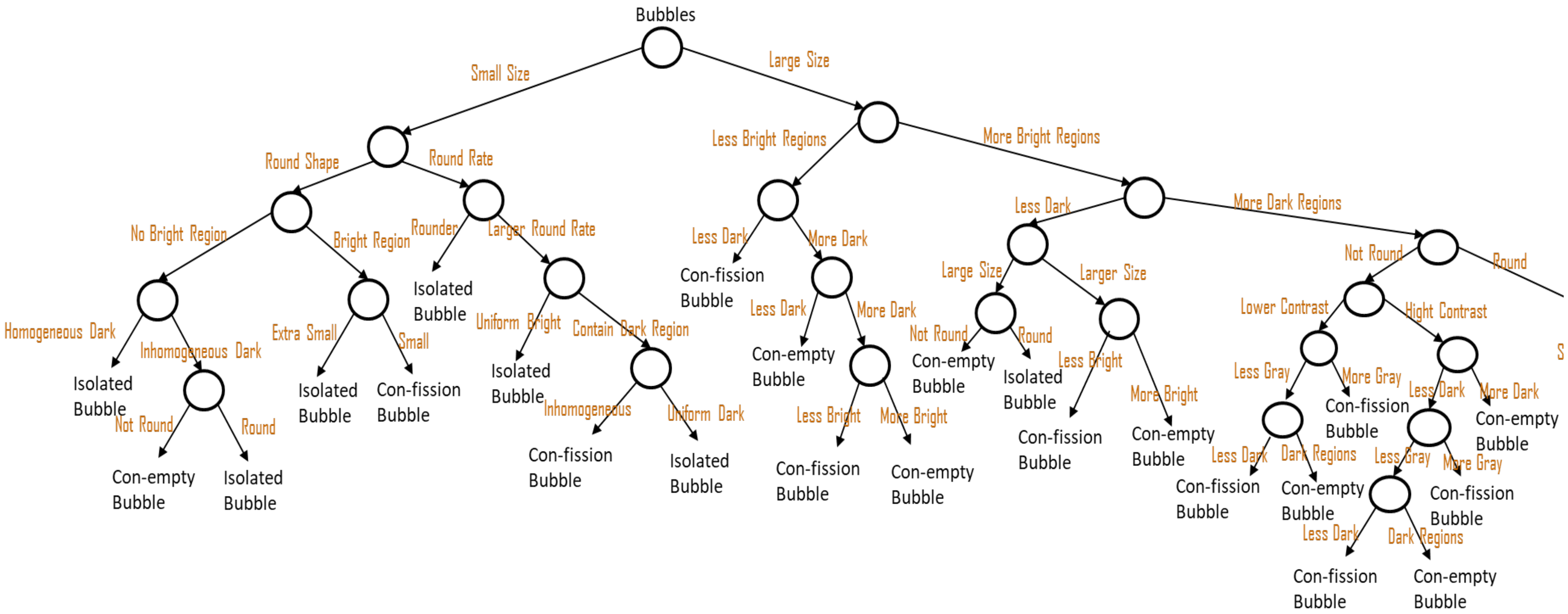

Fig. 1. Pre-trained decision tree model for fission gas bubble classification.

Quantitative insight to fission gas pores distribution (3/3)
Statistical analysis: Pore size distribution

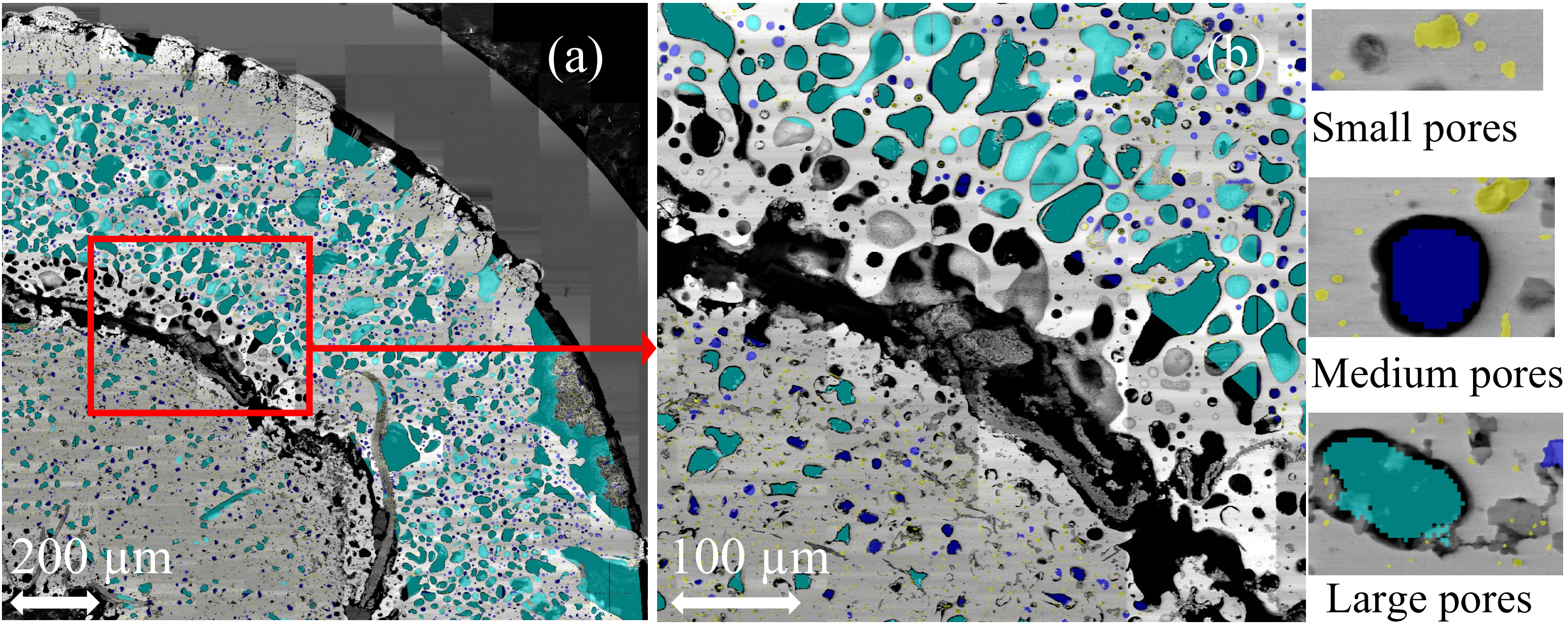

Fig. 1. Visualization of the pores with different sizes, (a) A quarter of the cross-section with area of interest, (b) Pores labeled using different colors.

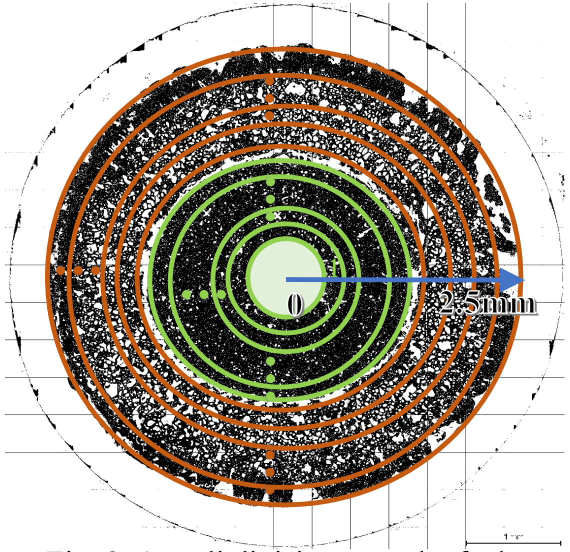

Fig. 2. Annuli division over the fuel cross section.

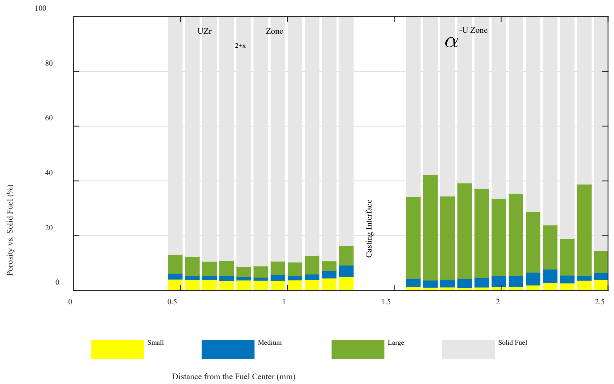

Fig. 3. The porosity distribution of different sizes over the whole cross section.

Quantitative insight to fission gas pores distribution (3/3)
Statistical analysis: Pore shape distribution

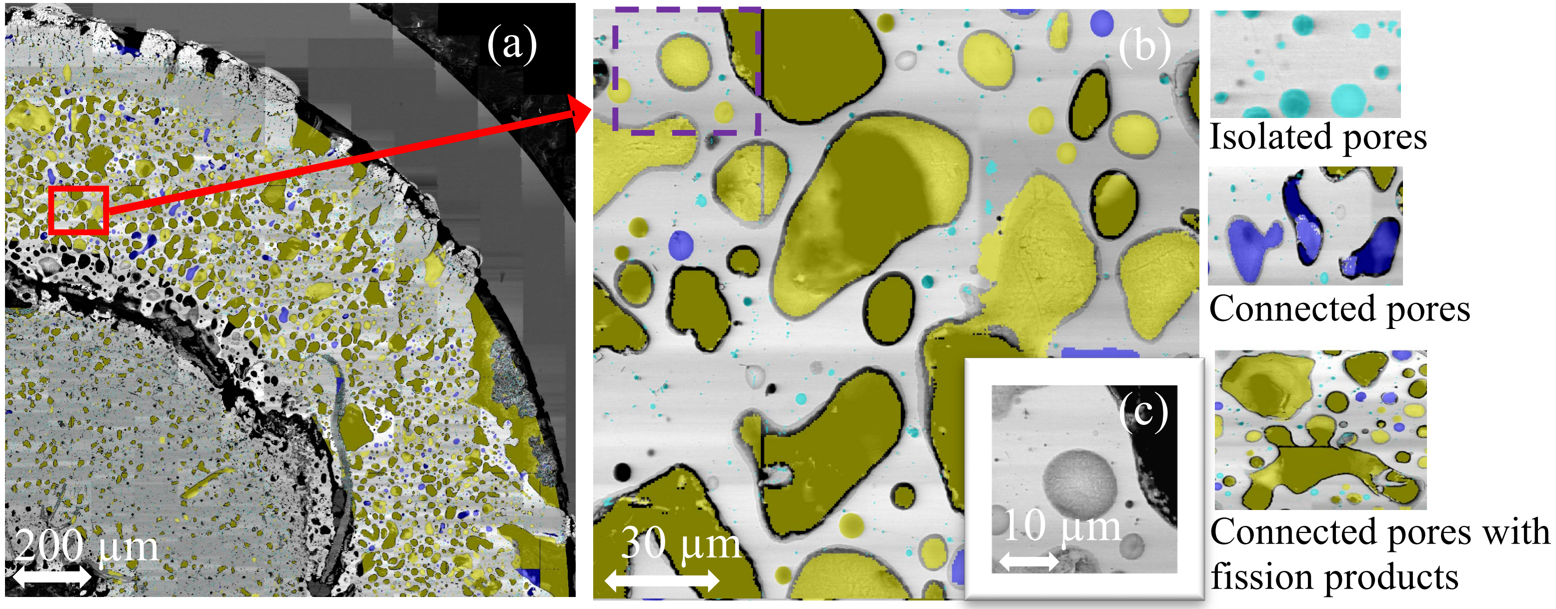

Fig. 1. Visualization of pore category classification result. (a) Overview showcasing distinct pore categories labeled in different colors; (b) Enlarged view of the region of interest marked in (a); (c) Original BSE image of the small round pore highlighted in (b).

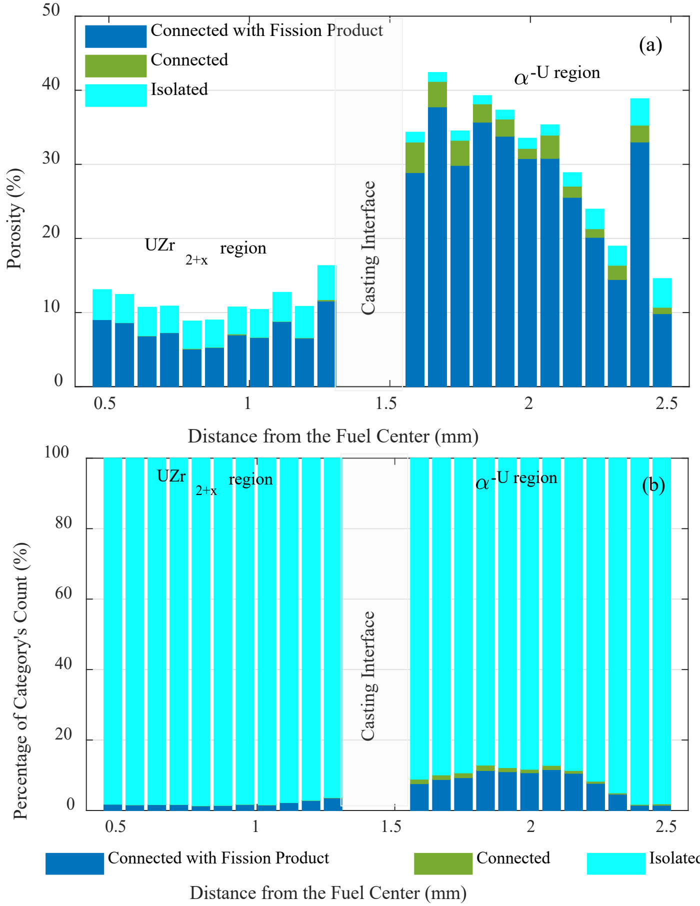

Fig. 2. (a)Porosity distribution of different shapes over the cross section;(b) Percentage of counts of different shapes over the cross section.

Pore orientation distribution

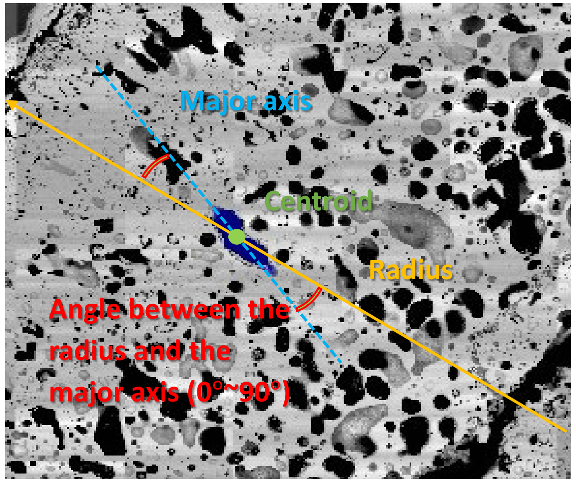

Fig. 1. Sketch of the pore orientation.

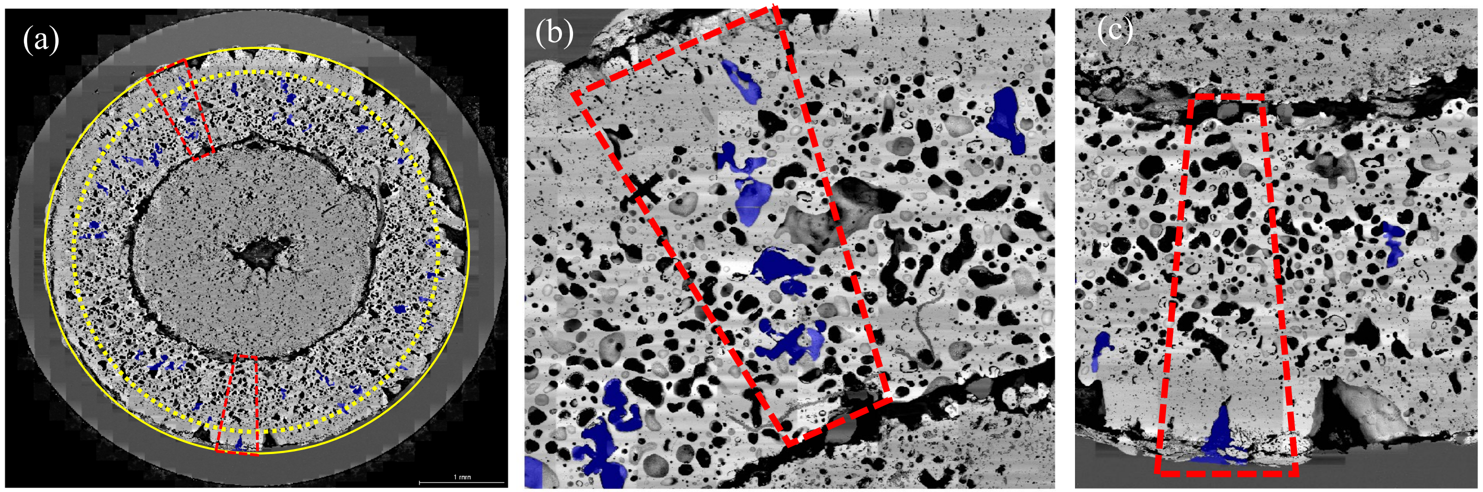

Fig. 2. Potential heat transfer pathways. (a) Cross-section marked with connected pores with the longest 5% major axis length and orientation within 30 degrees; (b) Potential continuous heat transfer path; (c) Discontinuous heat transfer path.

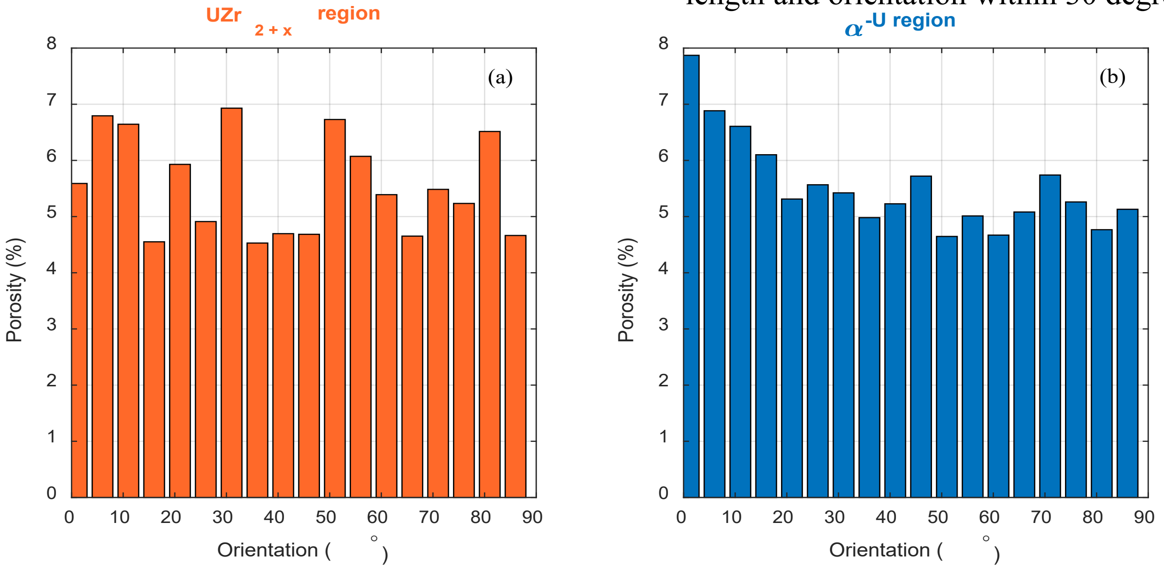

Fig. 3. Pore orientation distribution in UZr2 + x and α-U zones. (a)shows the porosity distribution based on orientations of the connected pores in the UZr_{2+x} zone; (b)shows the porosity distribution based on orientations of the connected pores in the α-U zone.

Conclusion

- Pore statistics were derived to better understand fuel performance such as the lanthanide migration and potential thermal conductivity degradation using machine learning.
- The porosity in the α-U zone was almost **3 times** of the UZr_{2+x} zone.
- In the α-U zone, large pores contributed to **83.47%** of the pores due to the growth of fission gas pore along the thermal gradient, and **94.3%** of the pore area was taken by connected pores.
- The morphology of porous structures is known to be related to the effective thermal conductivity of porous media.

Fission gas pores statistics

	Overall porosity	Small pore ($<32\mu m^2$)	Medium pore ($<205\mu m^2$)	Large pore ($\geq 205\mu m^2$)	Isolated pore	Connected-empty pore	Connected-fission product pore
Inner UZr_2 zone	11.13%	36.34%	17.11%	46.55%	34.50%	0.51%	64.99%
Outer α-U zone	32.66%	6.19%	10.34%	83.47%	5.71%	7.22%	87.07%

Acknowledgement

- This work was supported by the U.S. Department of Energy, Office of Nuclear Energy under DOE Idaho Operations Office.
- This research made use of the resources of the High Performance Computing Center at Idaho National Laboratory.
- The authors also acknowledge the support of DOE Advanced Fuel Campaign on the experimental data collection.
- Insightful discussion with Larry K Aagesen Jr. is also greatly appreciated.

Battelle Energy Alliance manages INL for the U.S. Department of Energy's Office of Nuclear Energy. INL is the nation's center for nuclear energy research and development, and also performs research in each of DOE's strategic goal areas: energy, national security, science and the environment.